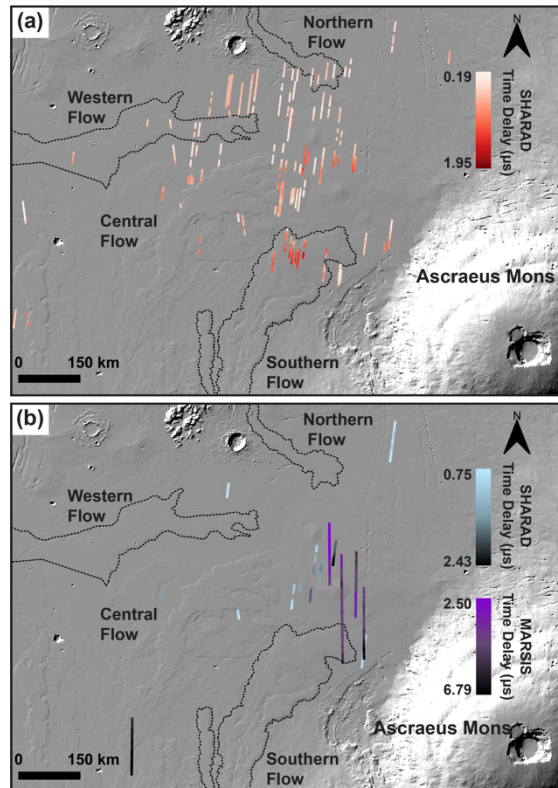


# **INVESTIGATING THE SUBSURFACE NORTHWEST OF ASCRAEUS MONS, MARS USING RADAR SOUNDING.** E. S. Shoemaker<sup>1</sup>, L. M. Carter<sup>1</sup>, W. B. Garry<sup>2</sup>, and G. A. Morgan<sup>3</sup>, <sup>1</sup>Lunar and Planetary Laboratory, University of Arizona, Tucson, AZ, <sup>2</sup>NASA Goddard Space Flight Center, Greenbelt, MD, <sup>3</sup>Planetary Science Institute, Tucson, AZ.

**Introduction:** The Tharsis volcanic province of Mars is host to the three large shield volcanoes that form a southwest-northeast chain through its center: Arsia Mons, Pavonis Mons, and Ascraeus Mons [1]. The Tharsis Montes are the source of extensive lava flows that are tens to hundreds of kilometers in length (Fig. 1) [2]. The morphology, composition, and spatial distribution of these lava flows provide insight into the evolution of the surface and interior of Mars.



**Figure 1.** Subsurface interfaces are detected within the margins of three flow complexes, mapped by [3], and throughout the surrounding plains at various two-way time delays. Margins of the three flow complexes with interfaces are outlined. Detected interfaces by SHARAD (panel a, red gradient) and b, blue gradient) and MARSIS (panel b, purple gradient) displayed on MOLA shaded relief map.

New coverage by SHARAD and reprocessed data from the Mars Advanced Radar for Subsurface and Ionospheric Sounding (MARSIS) [4] has allowed for an improved, in-depth survey of the Tharsis province that has revealed a more complex stratigraphy than previously recognized [5,6].

**Data and Methods:** We used the SHARAD and MARSIS radar sounders to survey northwest of Ascraeus Mons. SHARAD operates at a central

frequency of 20 MHz with a vertical resolution of 15 m in free space. MARSIS operates at 1.8, 3, 4, and 5 MHz. At 1 MHz, MARSIS has a vertical resolution of 150 m in free space [7]. Vertical resolution in the subsurface varies with the permittivity of different geologic materials [8]. SHARAD and MARSIS detect strong contrasts in permittivity in the subsurface that appear in the radargram at a greater time delay than the bright surface return (Fig. 2). Reflectors can be obscured by cross-track surface echoes which are identified by comparing the radargram to a simulation of surface clutter (cluttergram) produced using topography data obtained by the Mars Orbiter Laser Altimeter (MOLA) instrument (Fig. 2).

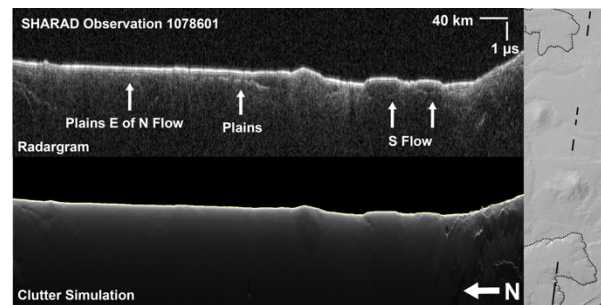


**Figure 2.** SHARAD radargrams indicate multiple reflectors beneath both volcanic plains and lava flows. **Top panel:** SHARAD observation 1078601. Along-track distance is in the x-direction and time delay is in the y-direction. **Bottom panel:** MOLA-derived clutter simulation.

Where a reflector appears to correlate with a lava flow visible in MOLA topography, we calculate the permittivity along each radar observation. We determine permittivity using a depth correction technique [9]. The surrounding volcanic plains demonstrate a very low slope and so we assume the lava flows are resting on a nearly flat surface. We connect the plains along the radar observation and adjust the depth of the interface to this line. We test permittivity values in the range reasonable for that of basalt ( $\epsilon' = 7-11$ ) [5,6,10] and produce new radargrams based on this range. The best match between these synthetic “depth corrected” radargrams and the subsurface provides the permittivity estimate. Mean thickness of the flow is determined from the permittivity of each SHARAD observations. Loss tangents were determined by breaking the SHARAD observations into 35 different groups based on their time-delay and locations. Multiple SHARAD tracks crossing a flow with optically or topographically visible boundaries were grouped together to produce a single loss tangent estimate for

that flow, while plains tracks were grouped based on time delay and proximity.

**Results:** We identified 11 SHARAD observations with interfaces that terminate at the margins of three distinct lava flows visible in MOLA topography: the Northern, Southern, and Western flows (Fig. 1, dashed lines). The remaining 35 SHARAD observations and five from MARSIS have interfaces associated with the surrounding volcanic plains. Average permittivity values for the three flows ranged from 8.0-10.7 corresponding to thicknesses of 26.4-52.5 m. The thinnest flow was the Western flow while the thickest was the Southern flow. The loss tangents for these flows were  $\sim 0.02$ -0.04. For the grouped SHARAD observations associated with the plains, thicknesses could not be estimated (no topographic surface expression), though their loss tangents ranged from  $\sim 0.01$ -0.07.

**Discussion and Conclusions:** SHARAD and MARSIS have detected a significant number of new reflectors in the Tharsis Province. Reflectors confined within the margin of three flows we interpret to be the base of that flow in contact with the surrounding volcanic plains. In several instances, deeper SHARAD reflectors (Fig. 1b) are at comparable time delays to identified MARSIS reflectors and the two instruments may be detecting the same stratigraphy. Determining the source of reflectors throughout the plains proves difficult since they lack correlation to surface topography. To aid in interpretation of stratigraphy in these regions, we compare outputs of an  $n$ -layer 1D forward model to real SHARAD outputs produced by [11]. User inputs include number of layers, thickness of  $n-1$  layers, permittivity and loss tangent of each layer. As an example, we model plains reflector 2509402 (Fig. 3a). This reflector is resting within an area mapped as ponded lava flows [3] confined by both the Southern flow complex and the fan-shaped deposits on the western flank of Ascraeus Mons. The model is highly dependent upon the contrast in permittivity, and so we consider two end-member scenarios with lower or higher permittivities for the lower layer compared to the upper layer, which we estimate to have a permittivity of 7.0 for basalt. An example of one of these outputs is shown in Fig. 3b. In this scenario a lower permittivity of 6.0 provides a best-fit to the SHARAD data. Based on the glacial activity in the region, this could potentially be sediment that has been covered by the lava comprising the upper layer in this model [12]. Alternatively, a low-density layer like pyroclastic material could have been deposited beneath this ponded lava to generate these reflectors [13].

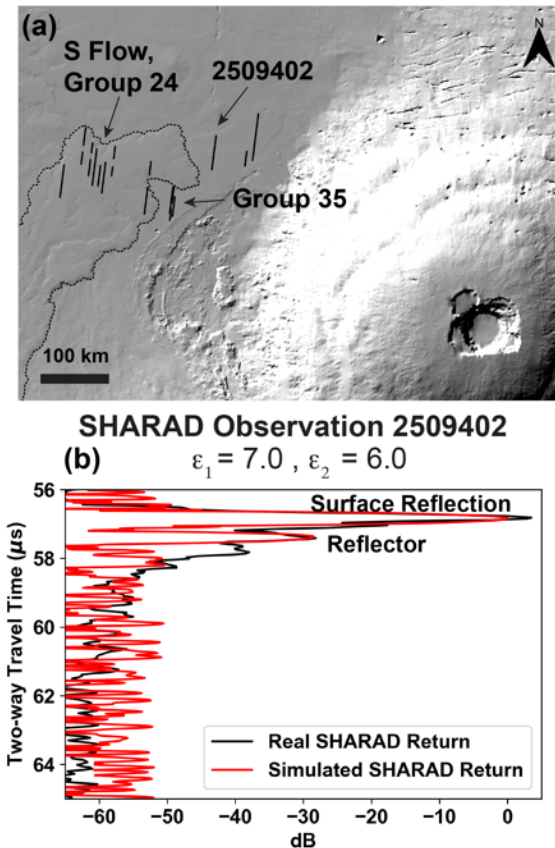


**Figure 3.** (a) SHARAD reflector 2509402 is within a mapped potential ponded lava unit within the fan-shaped deposits [3]. (b) Modeled SHARAD return for a lower density second layer, perhaps sediment or pyroclastic material [11,12,13].

**Acknowledgments:** SHARAD data obtained from NASA PDS. MARSIS data obtained from Colorado SHARAD Processing System (CO-SHARPS). This work was partially supported by a SHARAD Co-I grant to L. Carter.

**References:** [1]Crumpler, L. S., and Aubele, J. C. (1978) *Icarus*, 34, 496-511. [2]Garry, W. B., et al. (2007) *JGR*, 112(E8). [3]Mohr, K. J., et al. (2018), *Planet. Geol. Map. Mtg.*, No. 2066. [4]McMichael et al. (2017) *IEEE Radar Conf.*, 0873-0878. [5]Carter, L. M., et al. (2009a) *GRL*, 36, L23204. [6]Simon, M. N., et al. (2014) *JGR*, 119, 2291-2299. [7]Picardi, G., et al. (2004) *Planet. Space Sci.*, 52, 149-156. [8]Seu, R., et al. (2007) *JGR*, 112, E05S05. [9]Carter, L. M., et al. (2009b) *Icarus*, 199, 295-302. [10]Ulaby, F. T., et al. (1988) Rep. 23817-1-T, U. Mich. Rad. Lab. [11]Courville, S., et al. *in review*. [12]Kadish, S., et al. (2008) *Icarus*, 197(1), 84-109. [13]Ganesh, I., et al. (2020) *J. Volc. and Geo. Res.*, 390, 106748.